Supporting Information

Modification of $LiNi_{0.5}Mn_{1.5}O_4$ high potential cathode from the inner lattice to the outer surface with Cr^{3+}-doping and Li^+-conductor coating

Xiaojian Yang, Tao Yang, Shanshan Liang, Xin Wu and Hanping Zhang*

* *Jiangsu Key Laboratory of Advanced Catalytic Materials and Technology, Changzhou University, Changzhou 213164, China. E-mail: jinhongshi0001@163.com*

Experimental details

Sample preparation

All raw materials were analytical grade. For the preparation of $Li_{0.1}B_{0.967}PO_4$-coated $LiNi_{0.45}Cr_{0.1}Mn_{1.45}O_4$ (Cr-LNMO/LBPO) powders, 4 mmol of CH_3COOLi, 1.8 mmol of $Ni(NO_3)_2$, 5.8 mmol of $Mn(CH_3COO)_2$, 0.4 mmol of $Cr(NO_3)_3$ and 0.73 g of benzoyl peroxide (BPO) were dissolved in anhydrous ethanol under magnetic stirring, and then the resultant solution was evaporated at room temperature until a brown gel was obtained. The gel was placed in a crucible, then heated to 420 ^oC at a rate of 3 ^oC min^{-1} and held at that temperature for 3.5 h to release the volatile batch components. Subsequently, the residue was heated at 800 ^oC for 20 h at a rate of 5 ^oC min^{-1} and air cooled to room temperature. To coat Li^+ conductive layer on the surface of the obtained powders, stoichiometric amounts of $LiBO_2$, H_3BO_3 and $NH_4H_2PO_4$ were first completely dissolved in distilled water. Then these powders were slowly poured into the solution which was constantly stirred at 50 ^oC, accompanied by a slow evaporation of solvent. The resulting mass was heated sequentially, first at 110 ^oC for 3 h and next at 350 ^oC for 7 h to get final

product. The heating rate was 2 ^{o}C min^{-1} below 110 ^{o}C and 4 ^{o}C min^{-1} above 110 ^{o}C. The mass ratio of the nanosized coating material was controlled to be 1 wt%. The bare $LiNi_{0.5}Mn_{1.5}O_4$ (LNMO) and $LiNi_{0.45}Cr_{0.1}Mn_{1.45}O_4$ (Cr-LNMO) were prepared by the same procedure for comparison.

Structural characterization

X-ray diffraction (XRD) patterns were obtained using a Bruker D8 Focus power diffractometer (Cu-Kα, operation voltage: 40 kV, current: 25 mA). The surface morphologies of products were characterized by a JEOL JSM 6700F field emission scanning electron microscope (FESEM) coupled with an X-ray energy dispersive spectrometer (EDS). The structural analysis was conducted using a 200 kV JEOL IEM-2100F transmission electron microscope (TEM).

Electrochemical measurements

Electrochemical measurements were performed using CR2032 coin cells with lithium metal as counter and reference electrodes. 1M $LiPF_6$ in ethylene carbonate (EC)-dimethyl carbonate (DMC)-ethyl methyl carbonate (EMC) (1:1:1 in volume) was used as the electrolyte, and the separator was a polypropylene microporous film (Cellgard 2300). The cathodes were prepared by coating the homogeneous electrode slurry composed of dissolved 80 wt% as-synthesized materials, 10 wt% acetylene black and 10 wt% PVDF in N-methyl-2-pyrrolidone (NMP) on aluminum foil. The resulting film was dried at 80 ^{o}C for 12 h in vacuum to remove volatile solvent, and then cut into discs with a diameter of 5 mm and an active materials mass loading of 2.3 mg cm^{-2}. The disks were pressed under a pressure of 10 MPa. The cells were assembled in an argon-filled glovebox with H_2O and O_2 concentrations below 0.1 ppm and galvanostatically charged and discharged within the voltage range of 3.5 V to 4.95 V at room temperature. For the assessment of rate capability, the cell was charged at 1 C and discharged at different C rates from 1 to 50 C, where 1 C corresponds to 146 mA h g^{-1}. Cyclic voltammetric (CV) and

electrochemical impedance spectra (EIS) data were collected on a CHI660D electrochemical working station. CV curves were monitored at a scan rate of 0.1 mV s^{-1} within a voltage range of 3.5−4.95 V, and EIS spectra were obtained over a frequency range between 0.1 Hz and 65 kHz.

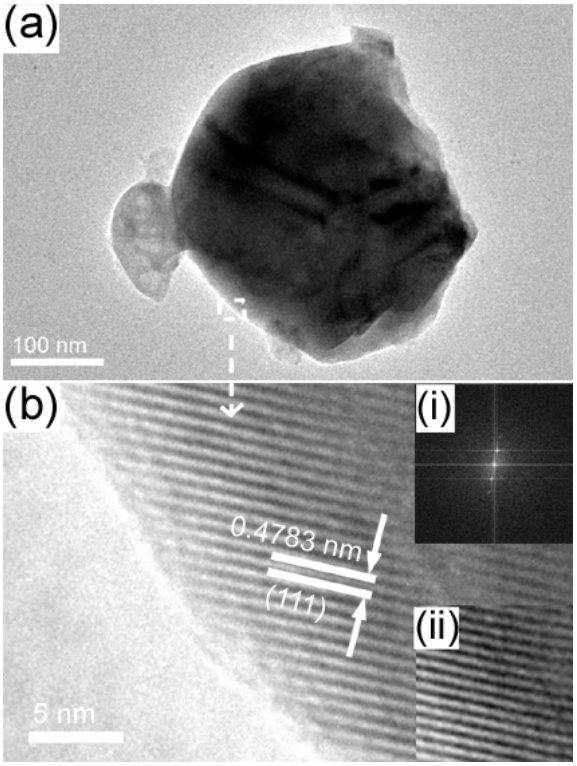

Figure S1. (a) TEM and (b) HRTEM images of LNMO. The inset (i) shows the Fast Fourier transformation (FFT) of the HRTEM image. The insert (ii) shows the Inverse FFT of insert (i).

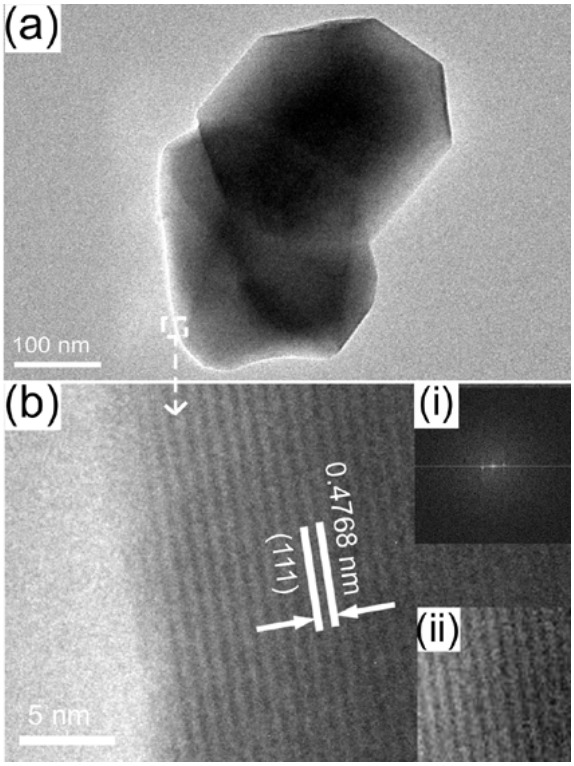

Figure S2. (a) TEM and (b) HRTEM images of Cr-LNMO. The insert (i) shows the FFT of the HRTEM image. The insert (ii) shows the Inverse FFT of insert (i).

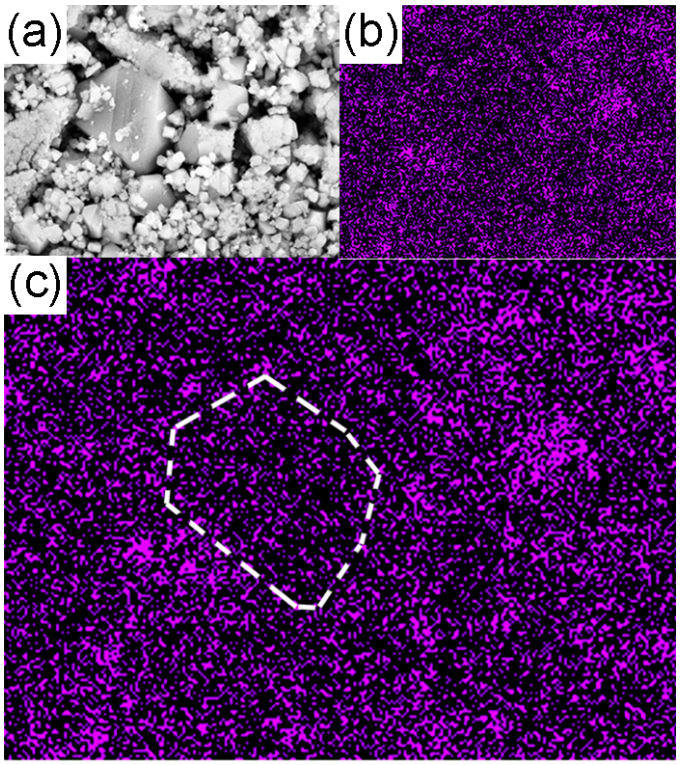

Figure S3. (a) FESEM image of the pressed pellet, (b) EDX elemental map for P in LBPO-Cr-LNMO, and (c) the zoom of (b). The dashed line in (c) outlines the dark area of the P map in (b) which roughly agrees with the geometry of the largest particle in (a).

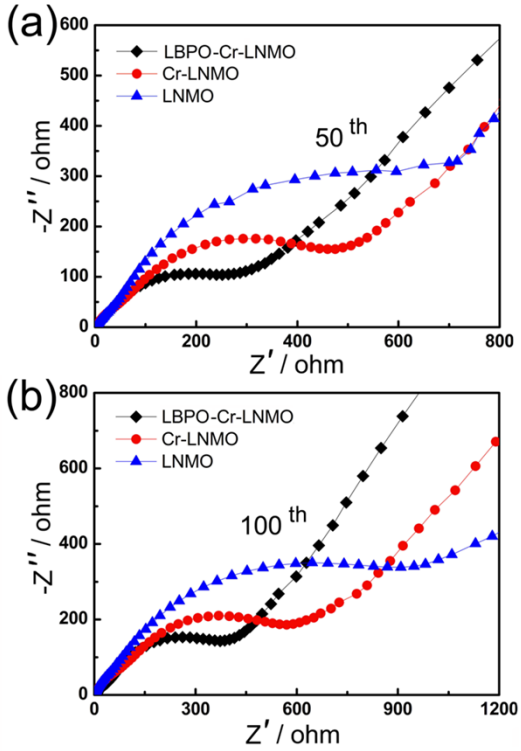

Figure S4. Nyquist plots of LNMO, Cr-LNMO and LBPO-Cr-LNMO with a frequency range from 65 kHz to 0.1 Hz at (a) the 50th and (b) the 100th cycle in the charged state at 4.95 V.

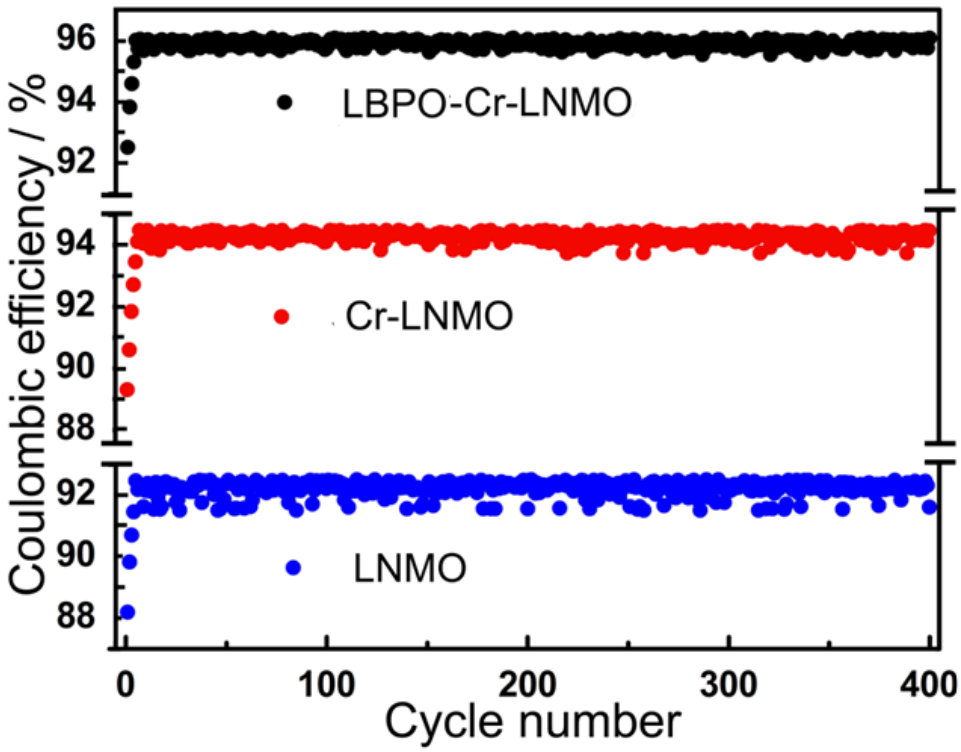

Figure S5. Coulombic efficiency of LNMO, Cr-LNMO and LBPO-Cr-LNMO at 1 C (146 mA h g^{-1}) between 3.5 and 4.95 V, respectively.

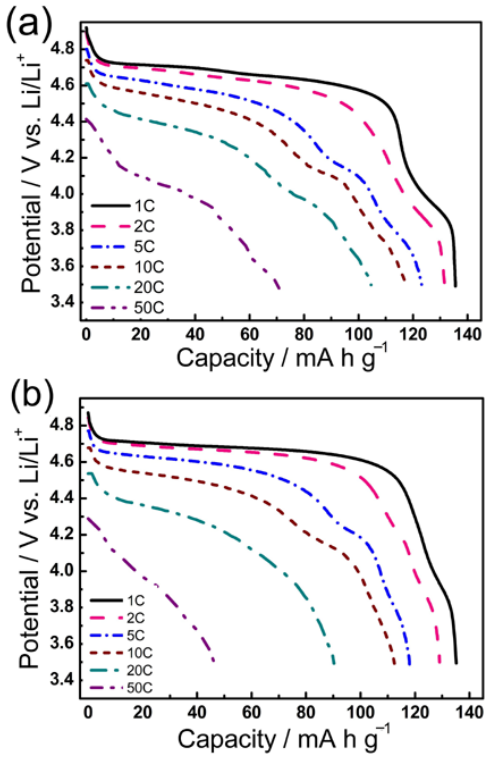

Figure S6. Discharge profiles of (a) LNMO and (b) Cr-LNMO at various rates between 3.5 and 4.95 V.

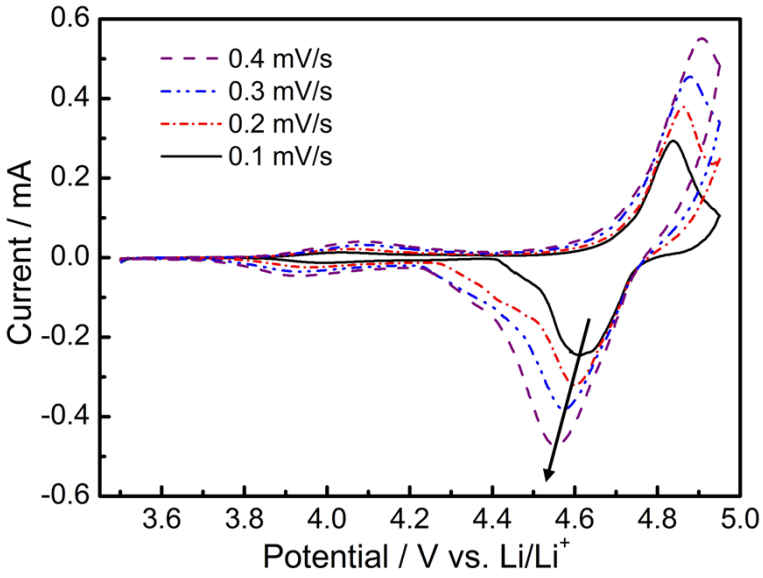

Figure S7. CV curves of bare LNMO at various scan rates.

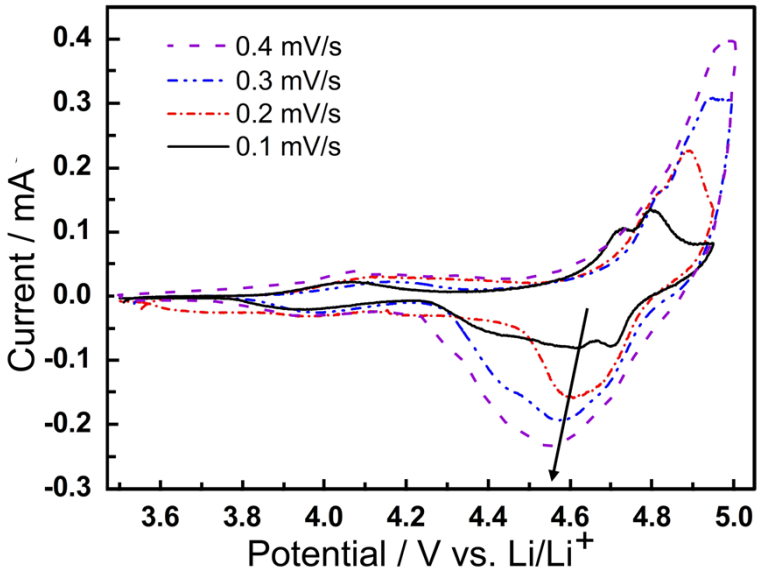

Figure S8. CV curves of Cr-LNMO at various scan rates.

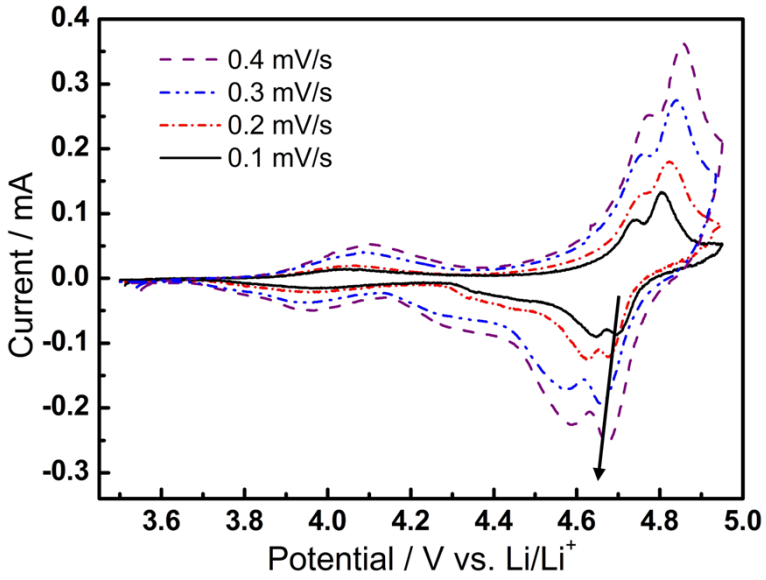

Figure S9. CV curves of LBPO-Cr-LNMO at various scan rates.

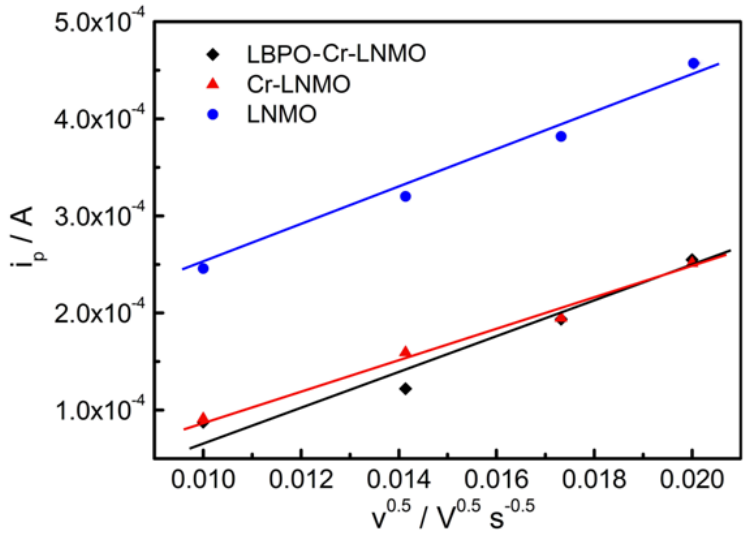

Figure S10. Plot of peak current (i_p) of the cyclic voltammograms vs. $v^{0.5}$. The v indicates the voltage scan rate.

From the slope of the linear fit, the Li^+ diffusion coefficients in three samples were calculated in the below equations:[1]

$$i_p = (2.69\times10^5)n^{1.5}AD^{0.5}\Delta C_o v^{0.5} \quad (1)$$

$$k = (2.69\times10^5)n^{1.5}AD^{0.5}\Delta C_o \quad (2)$$

$$\Delta C_o = C_{initial} - C_{final} \approx C_{initial} = \rho/M \quad (3)$$

Where i_p is the peak current, n is the number of electrons per reaction species (for Li^+ it is 1), A is the dipped area of the electrode into the electrolyte solution, D is the diffusion coefficient of Li^+ in the electrode, ΔC_o is the change in Li^+ concentration corresponding to specific electrochemical reaction, k is the slope of the linear fit, ρ is the density of active material, M is mole mass of active material.

Table S1. Various parameters in the equation (1), (2) and (3).

Symbol	n		A / cm^2		ρ / g cm^{-3}		M / g mol^{-1}
Value	1		0.196		1.76		182.69
Symbol	k_{LNMO}	D_{LNMO} / cm^2 s^{-1}	$k_{Cr\text{-}LNMO}$	$D_{Cr\text{-}LNMO}$ / cm^2 s^{-1}	$k_{LBPO\text{-}Cr\text{-}LNMO}$	$D_{LBPO\text{-}Cr\text{-}LNMO}$ / cm^2 s^{-1}	
Value	0.0155	9.29E−10	0.0169	1.10E−9	0.0194	1.46E−9	

Table S2. The fitted electrolyte resistances (R_e), surface film resistances (R_s) and charge transfer resistance (R_{ct}) for the Nyquist plots of LNMO, Cr-LNMO and LBPO-Cr-LNMO at the 1st cycle in the charged state at 4.95 V.

Sample	R_e		R_s		R_{ct}	
	Value /Ω	Error /%	Value /Ω	Error /%	Value /Ω	Error /%
LNMO	2.66	9.84	30.19	8.99	67.99	5.942
Cr-LNMO	3.93	7.89	42.93	5.45	158.2	4.09
LBPO-Cr-LNMO	3.84	8.2	43.58	5.79	179	4.18

Table S3. The fitted electrolyte resistances (R_e), surface film resistances (R_s) and charge transfer resistance (R_{ct}) for the Nyquist plots of LNMO, Cr-LNMO and LBPO-Cr-LNMO at the 50th cycle in the charged state of 4.95V.

Sample	R_e		R_s		R_{ct}	
	Value /Ω	Error /%	Value /Ω	Error /%	Value /Ω	Error /%
LNMO	4.10	4.77	21.71	8.48	150.4	3.58
Cr-LNMO	4.46	6.57	260	3.59	40.56	5.70
LBPO-Cr-LNMO	4.53	5.02	336.3	4.03	38.54	4.62

Table S4. The fitted electrolyte resistances (R_e), surface film resistances (R_s) and charge transfer resistance (R_{ct}) for the Nyquist plots of LNMO, Cr-LNMO and LBPO-Cr-LNMO at the 100th cycle in the charged state of 4.95 V.

Sample	R_e		R_s		R_{ct}	
	Value /Ω	Error /%	Value /Ω	Error /%	Value /Ω	Error /%
LNMO	6.67	5.238	190.3	4.34	26.24	6.25
Cr-LNMO	0.76	13.95	16.09	11.23	321.7	5.16
LBPO-Cr-LNMO	0.50	50.37	534.9	4.22	54.49	7.55

Reference

1 S. R. Das, S. B. Majumder and R. S. Katiyra, *J. Power Sources*, 2005, 139, 261-268.